Vol. 486: 13–22, 2013
doi: 10.3354/meps10374

MARINE ECOLOGY PROGRESS SERIES
Mar Ecol Prog Ser

Published July 12

Three-dimensional mapping of marine caves using a handheld echosounder

V. Gerovasileiou[1,*,], V. Trygonis[2,**], M. Sini[3], D. Koutsoubas[3], E. Voultsiadou[1]**

[1]Department of Zoology, School of Biology, Aristotle University of Thessaloniki, 54124 Thessaloniki, Greece
[2]Fisheries Management & Fisheries Acoustics Laboratory, Department of Marine Sciences, and [3]Marine Biodiversity & Coastal Management Laboratory, University of the Aegean, Mytilene 81100, Greece

ABSTRACT: Mapping survey sites is essential when studying the spatio-temporal distribution of sessile assemblages in submarine or semi-submerged marine caves. Acquiring the necessary topographic measurements is challenging, given that underwater mapping is performed in restricted spaces and with limited time or visibility. This study presents a rapid and cost-effective method for the 3-dimensional mapping and visualization of simple marine caves, where 'simple' mainly refers to the absence of a complex dendritic network of conduits. The method can be implemented by 2 divers using a regular dive line, an inexpensive handheld echosounder, and standard diving equipment. Source data are particularly compact and designed for ease of underwater acquisition, and post-survey processing is automatically performed by the accompanying customized software. The output is a scaled 3-dimensional model of the surveyed cave, which can be viewed from any particular orientation. It can be sliced to depict the horizontal zonation patterns of benthic assemblages, or used to extract approximate estimates of passage cross-sectional area. The method can assist the sampling design of ecological studies with minimum allocation of mapping resources and help the evaluation of topographic features that may affect the spatial distribution of marine biota.

KEY WORDS: Marine caves · Mapping · Topography · Zonation · Benthos

INTRODUCTION

Submarine, semi-submerged and anchihaline caves are an integral part of the rocky coastline, especially in regions with extended distribution of limestone (Lewin & Woodward 2009). Triggered by breakthrough developments in diving apparatus during the mid-1940s, several studies have investigated the faunal composition and community structure of marine caves (e.g. Pérès & Picard 1949, Laborel & Vacelet 1958, Riedl 1966) and reported on the spatio-temporal variability of cave-dwelling assemblages (Martí et al. 2004, Bussotti et al. 2006). Cave studies brought to light unique benthic communities of special scientific interest (Harmelin et al. 1985, Vacelet et al. 1994) and a previously unknown stygobiotic (cave-exclusive) fauna, particularly in anchihaline systems (Jaume & Boxshall 2005, Iliffe & Kornicker 2009). Marine caves have been identified as important biodiversity reservoirs (Gerovasileiou & Voultsiadou 2012) and there is evidence of temperature-induced changes in cave-dwelling communities, which include species that could be used as indicators for monitoring climate trends (Chevaldonné & Lejeusne 2003).

Topographic and physico-chemical characteristics of the seabed can significantly affect the spatial structure of marine biota. The development of species, assemblages and growth forms is influenced by depth (Garrabou et al. 2002), orientation (Dellow & Cassie 1955), slope (Bell & Barnes 2000a,b, Virgilio et al. 2006) and topographic complexity (Bell & Smith 2004), which can modify illumination, current flow, and sedimentation rate. Within caves, small-scale topographic variability induces sharp environmental gradients, generating spatial heterogeneity of benthic assemblages (Sará 1962, Benedetti-Cecchi et al. 1997).

*Email: vgerovas@bio.auth.gr
**These authors contributed equally to this work

It is thereby not surprising that virtually any attempt to study cavernicolous benthic communities includes a mapping component to produce a spatial model of the cave that puts the observed gradients in biological and abiotic parameters into context. Standard cave mapping methods include the measurement of inclination, bearing and length of passages, coupled with spatial information at selected stations that describes the distance to the cave walls (Worthington 1987). Data are then manually compiled to produce 2-dimensional (2D) cross-sections of the study area (Proctor & Smart 1989). Building upon the variety of survey methods, access points and hardware options available to terrestrial cave or groundwater channel mapping (e.g. Sellers & Chamberlain 1998, Poole et al. 2011), several software platforms have been developed for the generation of 3-dimensional (3D) cave models (see references in Boggus & Crawfis 2009 for a complete software list).

These modeling tools, however, are not properly adjusted for underwater biological sampling conditions, where hardware options, survey time, suitable reference points and data resolution are significantly limited. The goals and sampling scale of underwater biological cave research differ from terrestrial cave exploration endeavors. Research teams cannot always allocate the time and assets required by large-scale underwater mapping surveys (Am Ende 2001) or remotely operated options (e.g. Fairfield et al. 2007). *In situ* biological research in marine caves is logistically challenging and cave mapping has generally been accommodated by manually drawn 2D cross-sections of the study area (Onorato et al. 1999, Cicogna et al. 2003, Bussotti et al. 2006), while 3D aspects of the cave are rarely visualized (Gili et al. 1982). As demonstrated by Wunsch & Richter (1998) and Scheffers et al. (2003), researchers can greatly benefit from simple, inexpensive, easily implemented solutions for the exploration and rapid, digital reconstruction of coral reef cavities.

This study presents a rapid, cost-effective method for the 3D mapping and visualization of simple marine caves, where 'simple' mainly refers to the absence of a complex dendritic network of conduits and an overall shape that can be approximated as a series of successive passages. The method is applicable both to underwater and semi-submerged caves, has a minimum environmental footprint and can be implemented by 2 divers over 1 to 2 dedicated dives. It requires a regular dive line, an inexpensive handheld echosounder and standard diving equipment. The output is a scaled, digital, 3D representation of the surveyed cave, which can be manipulated into plan and profile views or used to extract approximate estimates of passage cross-sectional area.

MATERIALS AND METHODS

Rationale

Speed, cost-effectiveness and ease of underwater implementation are the main objectives. Therefore, mapping must be based on the minimum topological data that can be gathered manually and rapidly with off-the-shelf equipment. Moreover, given the narrow time margins and the physiological challenges associated with underwater surveys, the complexity of logged data and the amount of information that has to be relayed among divers must also be minimal. This implies that the reference points relative to which measurements are taken must be as intuitive to the divers as possible. The latter is of particular importance, considering that divers must concurrently gather data that are referenced to different coordinate systems: a Cartesian one that describes the direction and inclination of successive passages (as well as the divers' current position within the passage) and a polar coordinate system, centered on the diver, which facilitates measurement of the radial distances to passage walls at each increment along the mapping path. Assuming that caves will commonly have an inclination from horizontal (dip), a measurement system with 6 degrees of freedom is created that must be managed under adverse time or visibility conditions.

The proposed scheme is designed to reduce the logistics down to a few measurements that are easy to acquire, and to shift most of the complexity to the post-survey processing stage that is automatically performed by the accompanying software. The method's backbone is the establishment of a reference system using a regular dive line (rope) that is marked with distance indicators, which is stretched along the survey path starting from the cave entrance (Fig. 1). If the cave topography or length limits the use of a single rope, mapping is performed incrementally; after mapping the first segment, the reference rope is redeployed in a 'broken stick' fashion, i.e. the ending point of the initial rope is the starting point of the next. While swimming right next to the rope and at any arbitrary point along its length, the radial distance to the walls is measured with the handheld echosounder at angles which are easily determined empirically (e.g. top, left, bottom, right, corresponding to 0°, 90°, 180°, and 270°, respectively).

Mapping equipment

Next to standard SCUBA equipment, such as a magnetic compass and dive computer, the materials needed are (1) a dive reel with calibrated line, i.e. a lightweight and neutrally-buoyant rope with distance markers every 1 to 2 meters; (2) a Hondex PS-7 200 kHz portable echosounder or equivalent; (3) a tape measure as backup to the echosounder and (4) a dive slate. Floats and a waterproof range finder are also needed when mapping semi-submerged caves. A GPS device is necessary for recording the geographic coordinates of the cave when back at the sea surface.

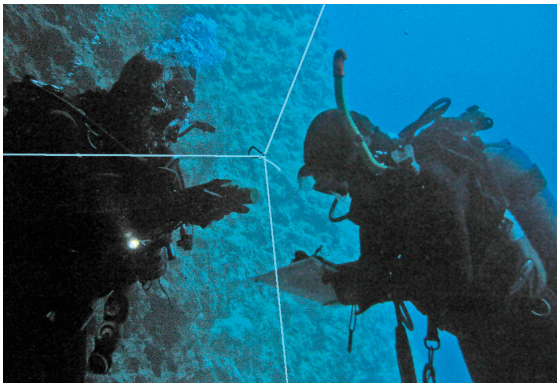

Fig. 1. Set up of the main coordinate system at the cave entrance. Two ropes are visible: the reference rope that runs across the cave and a secondary vertical line that spans from the sea surface to the entrance's floor, used only to provide a mounting basis. In the image, the diver on the left is acquiring a radial measurement at 0 m (distance on rope) and 90° angle (left), using the handheld echosounder

Process description (simulated data)

The mapping scheme was experimentally tested under field conditions on 3 marine caves located in the North Aegean Sea. In this section, simulated data are initially used for a step-by-step description of the method's implementation. This was done to illustrate aspects of the mapping scheme and source data requirements which were not necessarily fully exploited during the field surveys. The experimental layout and 3D models of the marine caves mapped during the actual field surveys are presented under 'Results'.

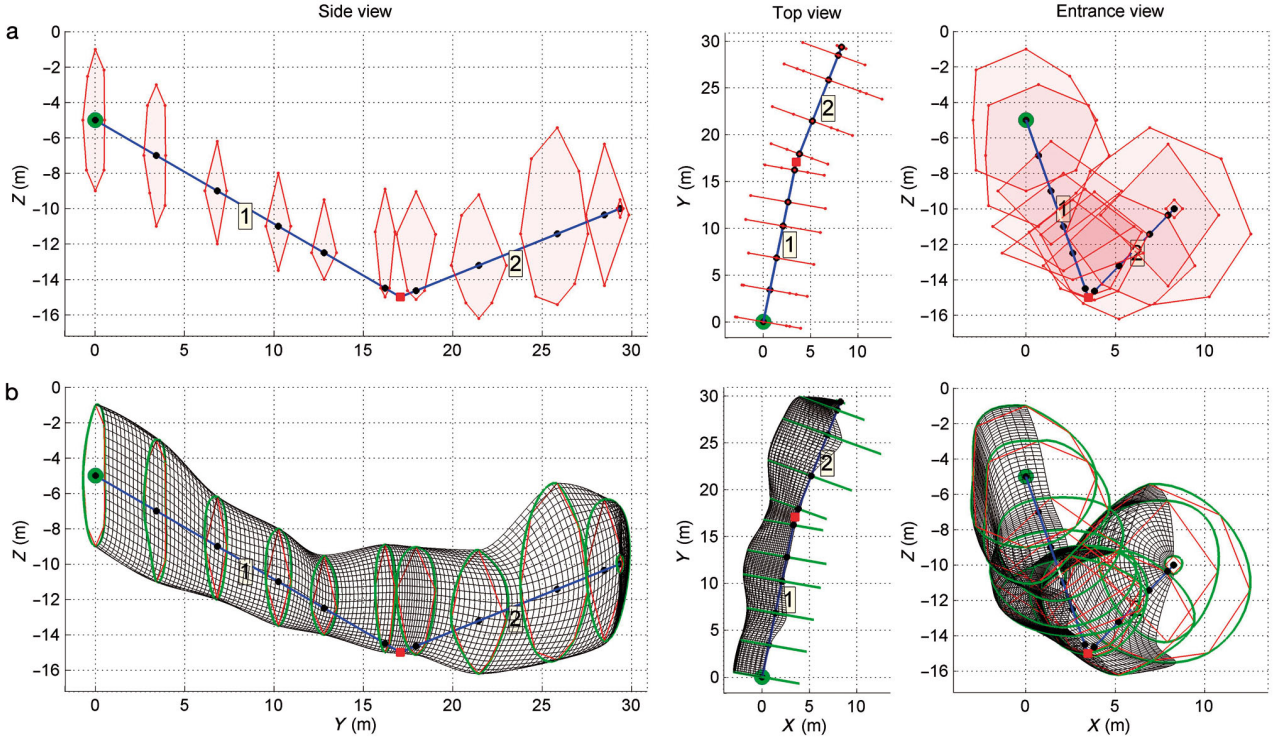

Fig. 2. Survey methods for rapidly mapping an underwater cave (simulated data). (a) The rope used for establishing the coordinate system is deployed in a 'broken stick' fashion (blue line), and cross-sectional measurements are acquired at chosen longitudinal intervals using the handheld echosounder (red patches). The green marker denotes the cave entrance and the red square represents the splitting node. Annotation numbers '1' and '2' are the unique rope IDs, marking the different ropes used. (b) The processing software parses the survey data and automatically creates the 3D mesh, while preserving the scale, depth, azimuth, and inclination of cave passages. Source data are listed in Table 1

Table 1. Source data for creating the cave model depicted in Fig. 2 (simulated cave). The first 7 columns are rope metadata; note that parent ID is always 0 for the root rope. The last 8 columns are the echosounder radial measurements across 8 possible angles. Angles for which no measurement was taken are left blank

Rope ID	Start depth (m)	End depth (m)	Bearing (° relative to north)	Parent ID	Rope length (m)	Distance on rope (m)	Angle of radial measurement (°)							
							0	45	90	135	180	225	270	315
1	–5	–15	10	0	20	0	4	4	3	4	4	4	4	3.5
1						4	4	4	3	4	4	3	4	4
1						8	2.8		3		3		4	
1						12	3		4		2.5		4	
1						15	3		4		1.5		4	
1						19	5.6	4.5	1.4		0.5		1.4	4.5
2		–10	20	1	14	1	5.6	4.5	1.4		0.5		1.4	4.5
2						5	4		4.5	3	3	3	4.5	4
2						10	6	5	5	4	4	5	6	6
2						13	4		4		4		3	
2						14	0.1		0.1		0.1		0.1	

The simulated scenario entails the mapping of a 30 m long, fully submerged cave with one entrance, consisting of 2 successive passages. The survey is performed by 2 divers and is accomplished over 2 separate dives. The sampling layout is shown in Fig. 2a, and Table 1 lists the full extent of topographic measurements, formatted exactly as required by the processing software.

The first dive is dedicated to a preliminary investigation of the survey site. Given that the underwater cave may not offer a line-of-sight connection between its entrance and innermost point (Fig. 2), mapping is performed by splitting the survey path into 2 consecutive segments. An intermediate station along the cave is identified as the splitting node according to the following criteria: (1) the point offers line-of-sight with both ends of the cave, (2) it provides convenient ground for securing the rope, and (3) selection of the point's location is such that it does not result in overlapping cross-sectional measurements, which are not supported by the processing software. Cave wall complexity is also assessed, in order to identify areas with abrupt local changes in topography that require higher sampling resolution.

On the follow-up dive, the mapping survey starts from the cave entrance where the first objective is to establish the zero reference point. During descent, a regular dive line is deployed that spans from the sea surface to the cave entrance in order to provide a mounting point for the reference rope (Fig. 1). Alternatively, the mounting line can be fixed on 2 points across the cave entrance. Diver 1 secures one end of the reference rope on the mounting line, while Diver 2 swims inside the cave and towards the predefined intermediate node, holding the other end of the rope. Once the rope is stretched along the passage and fixed on both ends, only 4 straightforward measurements are required to fully define the rope's 3D position in space (Table 1): Diver 1 logs the rope start depth (–5 m) and bearing relative to north (10°), while Diver 2 logs the rope end depth (–15 m) and start-to-end length (20 m). The latter is readily determined by the distance indicators that run along the rope.

With the coordinate system in place, the divers meet up at the cave entrance to start logging the radial measurements. These are acquired by swimming along the rope (following its inclination) and stopping at any arbitrary interval, based on the desired longitudinal resolution. In this example, 6 cross-sections were mapped for the first passage (Fig. 2a), spaced at intervals that ranged from 1 to 5 meters. Note that the last cross-section was acquired 1 m before the rope end (distance on rope = 19 m, Table 1), in order to avoid an overlapping measurement with the first cross-section of the upcoming rope deployment. Cross-sections are always mapped on a plane perpendicular to the sea surface, irrespective of rope inclination (Fig. 2a, top view), which significantly simplifies and speeds up data acquisition. In practical terms, the handheld echosounder is held on the vertical plane, and pointed at various angles. A maximum of 8 angles per cross-section are supported: top, left, bottom, right, as well as 4 in-between angles. These angles can all be easily determined empirically underwater. Any combination of angles may be selected according to the desired resolution per cross-section, as indicated by the missing radial measurements in Table 1. This adds to the overall flexibility of the method. For each cross-section, logged data are limited to the radial measurements and the distance

along the rope where these measurements were taken, counting from the rope start.

After mapping the first cave passage, the reference rope (or a second one if available) is redeployed along the second cave segment in a 'broken stick' manner (Fig. 2), i.e. the second rope (child) starts exactly where the initial rope (parent) ended. This parent-child hierarchy minimizes the number of measurements needed to position the new rope in 3D space, and references all new cross-sectional measurements back to the cave entrance. For any child rope, divers only have to measure the new bearing (20°), end depth (–10 m), and start-to-end length (14 m, Table 1). Start depth is automatically determined by the processing software based on rope connectivity, and is not required for child ropes. Cross-section mapping is then performed according to the described procedures. When back at the surface, the geographic coordinates of the cave entrance are logged using a regular GPS device.

Post-survey processing

Data processing and visualization are performed with a custom software script written in MATLAB (Mathworks), which is provided in the Supplement at www.int-res.com/articles/suppl/m486p013_supp/. The only input data required are the topographic measurements of Table 1, formatted as displayed therein and saved as a standard MS Excel file, including the table's headers. If a single rope was used for mapping the cave, the lines corresponding to rope 2 are removed from the source file; for more than 2 ropes, extra lines are added in a similar format. The main formatting requirements are that the initial (root) rope, which is placed at the cave entrance, must appear first in the data table, and that parent ropes are listed prior to their children.

Data analysis is a 3 stage process, involving the reconstruction of the cave geometry based on the actual measurements, the interpolation of these measurements to create the basis for the exterior 3D mesh, and the visualization of the final model including all intermediate steps. All 3 stages are automatically computed, requiring no user intervention. The software initially parses the data file and determines the total number of ropes used, their direction and inclination, as well as their connectivity. A Cartesian coordinate system is established, where the positive x-axis points east, the positive y-axis points north (magnetic), and the z-axis represents depth, with zero at the sea surface and negative values underwater (Fig. 2b). The starting point of the root rope is fixed at $(x, y, z) = (0, 0, z_s)$, where z_s is the rope starting depth, and ropes are sequentially positioned in space according to their connectivity, bearing, length, and inclination. This produces a simple line map, i.e. a scaled representation of the cave as a series of inter-connected line branches. Starting from the cave entrance and walking along each rope, the software then resolves the geometry of the radial measurements and positions the cross-sections accordingly. Each cross-section is interpolated using parametric splines that create a smoothed closed curve that follows the empirical radial measurements, and a 3D mesh is created around the cave by joining the successive cross-sections. The mesh is then refined to produce the final model (Fig. 2b).

RESULTS

Three marine caves situated in Lesvos and Agios Efstratios islands, North Aegean Sea, were used to test the validity and repeatability of the mapping scheme. Agios Vasilios (38°58′ 13.25″ N, 26°32′ 30.46″ E) and Fara (38°58′ 11.64″ N, 26°28′ 39.54″ E) are totally submerged caves at an average depth of 30 and 14 m respectively, whereas Ftelio (39°30′ 13.74″ N, 24°58′ 16.44″ E) is a shallow semi-submerged cave with a narrow entrance, ending in a larger chamber with an internal shore (Fig. 3a–c). Each cave was mapped over the course of 2 dives using a single rope deployment. The rope was stretched at sea level in the semi-submerged Ftelio cave and distance to the ceiling was measured with a range finder. For all caves, a maximum of 5 radial measurements were logged per cross-section. These were acquired at longitudinal intervals that varied from 0.5 to 5 m, depending on the local topographic complexity. Overall, a total of 9, 10, and 19 cross-sections were measured for Agios Vasilios, Fara, and Ftelio, respectively (Fig. 3).

The final 3D models of the surveyed caves are shown in Fig. 4. These were produced using the accompanying MATLAB-based processing script. Each model is scaled and can be viewed from any particular orientation in space, or sliced to illustrate the internal cave morphology (Fig. 4d–e). Alongside the final 3D model, the software also renders all intermediate topographic data and processing steps, starting with the reference rope and building up to the raw radial measurements and the interpolated cross-sections, as well as the initial mesh prior to its final refinement.

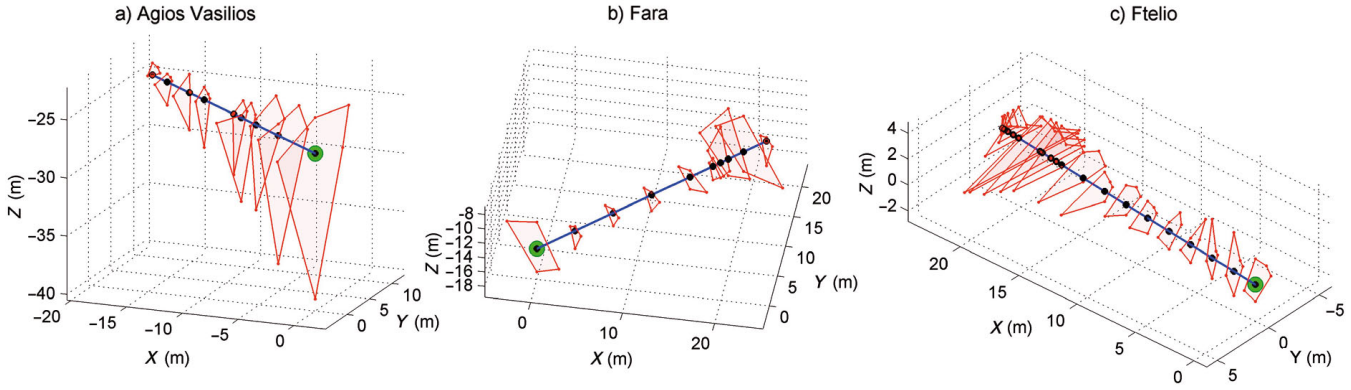

Fig. 3. Topographic measurements used for mapping the 3 North Aegean marine caves. The single rope used for establishing the coordinate system is denoted by the blue line. The red patches indicate the cross-sectional measurements, and the green marker shows the cave entrance. The positive *y*-axis points due north. Scale differs among subplots

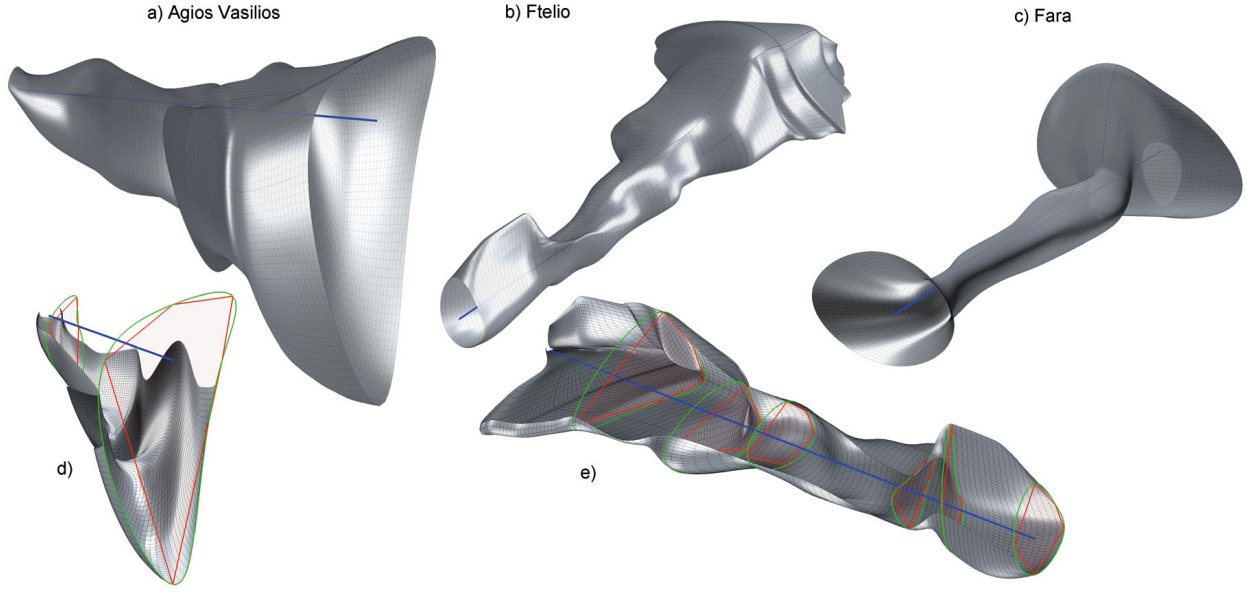

Fig. 4. Three-dimensional models (a–c) of the surveyed marine caves, (d–e) sliced to illustrate details of the internal morphology. Rope length (blue line) is 22, 23.5, and 30 m for Agios Vasilios, Ftelio, and Fara, respectively. Scale differs among models

In addition to providing a scaled representation of the surveyed cave, the 3D model can also be used to depict particular biological features on the corresponding wall sectors. As an example, a sliced model of Agios Vasilios cave is shown in Fig. 5, where the horizontal biological zonation of benthic assemblages along the entrance–interior axis is visualized, using data from a broader biological study performed at the surveyed marine caves (V. Gerovasileiou & E. Voultsiadou unpubl.). The cross-sectional area at various longitudinal distances along the cave is also computed automatically (Fig. 5, inset).

DISCUSSION

Topographic complexity is a key factor affecting the distribution of biota in underwater environments. Marine caves in particular often host localized pockets of organisms, which are either absent from or exist only sparsely in nearby locations (Roff & Zacharias 2011). The local presence of strong physicochemical gradients is reflected in patterns of biological spatial variability that is manifested as distinct zones within the cave (Riedl 1966). These patterns typically differ among and within caves, thus resulting in a wide variety of cave environments that are

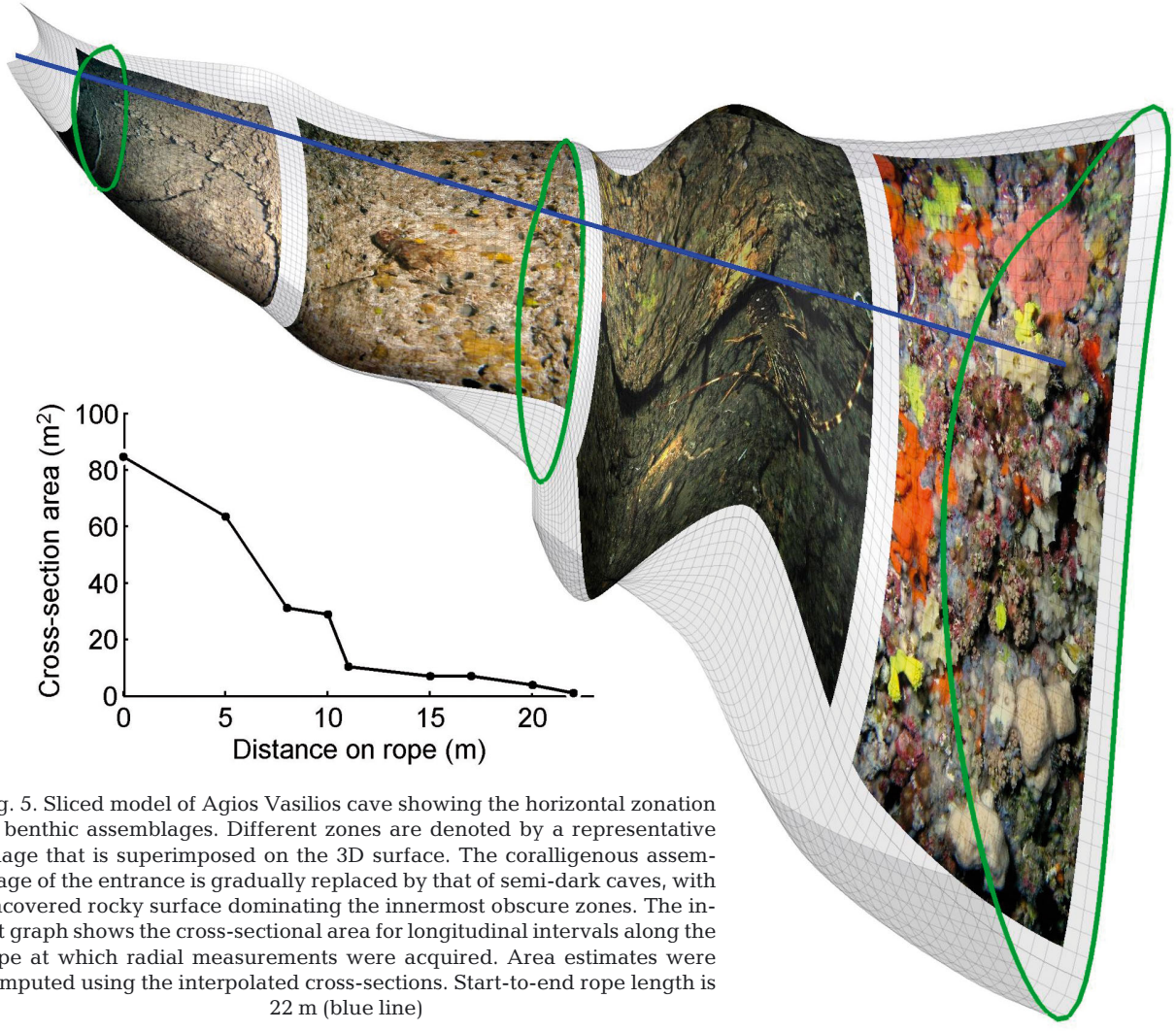

Fig. 5. Sliced model of Agios Vasilios cave showing the horizontal zonation in benthic assemblages. Different zones are denoted by a representative image that is superimposed on the 3D surface. The coralligenous assemblage of the entrance is gradually replaced by that of semi-dark caves, with uncovered rocky surface dominating the innermost obscure zones. The inset graph shows the cross-sectional area for longitudinal intervals along the rope at which radial measurements were acquired. Area estimates were computed using the interpolated cross-sections. Start-to-end rope length is 22 m (blue line)

characterized by high levels of individuality (see Bussotti et al. 2006 and references therein for details). Therefore, the commonly used exterior–interior zonation scheme may not always be an effective approach for all cave types (Parravicini et al. 2010), and a description of the cave topography prior to the actual survey can greatly assist the sampling design. While light is the determining abiotic parameter for algal communities near the entrance, animal-dominated communities inside the cave seem to be mainly dependent upon the site-specific geomorphology (Martí et al. 2004). Topography-induced changes in abiotic parameters and associated modifications in food or larval supply have a variable effect on the distribution of different sessile invertebrate assemblages (Riedl 1966), as well as their morphology and structural complexity within a cave (Pouliquen 1972, Zibrowius 1978, Bell 2002). The exact mechanisms underlying this biological spatial variability are poorly understood (Benedetti-Cecchi et al. 1997, Martí et al. 2004), but there is general consensus that ecological interactions need to be examined in the particular topographic context.

The described method directly addresses this need, by providing an adaptable mapping scheme for producing a realistic representation of the underwater cave in a rapid and cost-effective manner. As demonstrated by the field trials, the method is applicable both to fully and semi-submerged marine caves, requiring a small number of dedicated dives and readily available equipment. The resulting 3D models can help the evaluation of particular topographic features or overall cave morphology that may be driving the observed composition and spatial distribution of marine biota. Fichez (1990) suggested a direct connection between the cave profile and the horizontal stratification of water masses that created oligotrophic conditions at specific sectors of the cave.

Further studies showed that a descending floor profile may indicate entrapment of cold water, which, when combined with the darkness of the inner sectors, simulates deep-sea conditions even in shallow water caves (Vacelet et al. 1994, Harmelin & Vacelet 1997). These important attributes of the survey site can be assessed directly with this cost-effective method, given that the cave is drawn to scale and at its natural inclination, while the depth coordinates (i.e. slope) of the ceiling and floor profiles can be readily extracted from the respective longitudinal slices (see Fig. 2b). Contrary to a 2D schematic of the cave, a 3D model can illustrate more clearly whether a particular cave sector — or the entire cave morphology — functions as a sediment trap, thus explaining the local presence of distinct benthic communities (Zabala & Gili 1985, Bibiloni et al. 1989). Cross-sectional area and orientation of cave passages are also provided, which can be combined with additional *in situ* measurements of water flow or illumination to quantitatively examine the effects of abiotic parameters and local cave morphology on the ecological patterns observed.

Capitalizing on the versatility of computer-generated graphics, the cave models can be rendered to depict the particular biological assemblages characterizing each sector (Fig. 5) or be sliced to reveal details of the internal morphology that are difficult to review in 2D, such as walls with negative inclination and overhangs. These features of topographic heterogeneity affect illumination levels locally, with overhanging walls and cave ceilings supporting more sciaphilic assemblages than the sub-vertical and horizontal ones (Laborel & Vacelet 1958). The 3D representation of the survey site provides a valuable basis for the monitoring of individual caves over time and enhances the dissemination of scientific results to the wider community.

Source data are particularly compact and carefully selected for ease of underwater acquisition. The coordinate system is established mainly through measurements of depth and length, which are easily acquired using the dive computer and by visual inspection of the rope distance markers, respectively. The only angle measurement required is the rope bearing that is determined with a compass. The inclination angle, which is harder to ascertain, is completely ignored during the underwater survey and is determined by the processing software via the rope start depth, end depth, and start-to-end length. Moreover, the reference rope does not have to be centered on the cave axis, nor follow the actual inclination of the cave, as illustrated in Fig. 2. Divers are free to establish a rope layout that is adapted to the particular site, while leaving all geometric calculations to the processing software. The handheld echosounder provides a convenient means of acquiring radial distances, but can easily be replaced by a tape measure in cave sectors where the rugged wall morphology hinders reliable acoustic measurements. Equally important is that the scheme allows the *in situ* determination of required resolution, allowing the divers to adjust both the longitudinal intervals and the detail in angular measurements during the actual sampling dive. In our field surveys, a moderate number of 9 to 19 cross-sections were necessary to depict the caves adequately with a maximum of 5 angular measurements per cross-section. Longitudinal resolution was higher (1 m) in areas of abrupt local changes in topography and lower (4 to 5 m) in the smoother cave sections.

In terms of source data maintenance, the cross-sections that need special attention are those at the innermost wall, at the intermediate node (if more than one rope is used), and at sections where the cave has abrupt changes in bearing, i.e. at steep curves. Specifically, a phantom cross-section with small radial measurements is required at the innermost wall in order for the mesh to close properly (see the last row in Table 1). Also, radial measurements close to rope nodes or steep curves must be spaced close enough so that the model can follow the curve realistically, but cross-sections must not overlap, given that the mesh is constructed by connecting the successive cross-sections. These constraints are assessed during the preparatory dive, but manual corrections can be applied during post-survey processing.

Although able to rapidly produce a scaled model that is valuable for assessing the local effects of topography on hard substrate biota, the presented mapping scheme is not designed for fine-scale accuracy. Being a manual implementation, the method is prone to errors associated both with the position of divers within the cave and the position of measuring equipment (echosounder, tape measure or range finder) relative to the rope axis. Crude estimates of the longitudinal distance at which a cross-section was measured introduce bias into the cave model, while not adequately stretching the reference rope also has a negative effect on the output. Although it is theoretically feasible to map particularly long caves, the practicality of the method in such cases is limited, considering the logistics of managing the successive ropes accurately and the accumulation of

errors over repeated rope deployments. The latter, however, is not particular to this method, but rather embedded in any cave mapping effort where there is no means of acquiring intermediate reference points objectively. Am Ende (2001) used magnetic beacons and dedicated surface teams to periodically reset the respective errors, but this approach is clearly beyond the specifications of a rapid and cost-effective mapping scheme. Future experiments with controlled variability in sampling configurations would help to quantify the relative importance of the aforementioned parameters.

The accuracy of produced cross-sections depends on the number of radial measurements, which is limited to 8 possible entries per cross-section. This number and the radial directions were purposely selected to serve the rapid and manual implementation objectives, but this directly imposes an upper limit in the maximum resolution achievable. However, considering the typically large beam width of handheld echosounders (20 to 30°) and that the acoustic beam spreads with distance, increasing the number of radial measurements does not necessarily improve the output resolution. Unless acquired at a short distance from the wall, closely-spaced successive radial measurements practically overlap.

The method can benefit from future improvements that would allow the mapping of vertical passages and caves of complex morphology with multiple junctions. The latter requires a more elaborate underwater management of the manually established coordinate system and a different approach in data processing. In the current implementation, the mesh is created by joining the successive cross-sections; this allows a computationally inexpensive and unsupervised reconstruction of the cave model, but cannot handle the depiction of junctions. Heuristic algorithms for reconstructing a 3D object from a non-gridded cloud of point measurements are available (e.g. Bernardini & Bajaj 1997, Bernardini et al. 1999, Amenta et al. 2001, Holenstein et al. 2011), yet their implementation is challenging where source data are noisy or extremely sparse. Ultimately, increasing underwater site complexity compromises the use of manual and cost-effective sampling approaches. Moreover, complex sites are likely to require a higher degree of user intervention during the site-specific post-survey processing stage. Although the method presented here is not able to handle all types of underwater sites, it provides an easily implemented mapping solution to a variety of marine caves, facilitating the study of cavernicolous hard-substrate communities.

Acknowledgements. The authors thank E. Akritopoulou for her valuable help during the fieldwork. This research has been co-financed (January 2011 up to date) by the European Union (European Social Fund) and Greek national funds through the operational program 'Education and Lifelong Learning' of the National Strategic Reference Framework research funding program 'Heracleitus II: Investing in knowledge society through the European Social Fund'. V.G. also benefited from an Alexander S. Onassis Public Benefit Foundation fellowship for postgraduate studies (October 2009 to December 2010).

LITERATURE CITED

Am Ende BA (2001) 3D mapping of underwater caves. IEEE Comput Graph Appl 21:14–20

Amenta N, Choi S, Dey TK, Leekha N (2001) The power crust. Proc 6th ACM Symp Sol Mod App, 4–8 Jun, Ann Arbor, MI, p 249–260

Bell JJ (2002) The sponge community in a semi-submerged temperate sea cave: density, diversity and richness. PSZN I: Mar Ecol 23:297–311

Bell JJ, Barnes DKA (2000a) The distribution and prevalence of sponges in relation to environmental gradients within a temperate sea lough: inclined cliff surfaces. Divers Distrib 6:305–323

Bell JJ, Barnes DKA (2000b) The distribution and prevalence of sponges in relation to environmental gradients within a temperate sea lough: vertical cliff surfaces. Divers Distrib 6:283–303

Bell JJ, Smith D (2004) Ecology of sponge assemblages (Porifera) in the Wakatobi region, south-east Sulawesi, Indonesia: richness and abundance. J Mar Biol Assoc UK 84:581–591

Benedetti-Cecchi L, Airoldi L, Abbiati M, Cinelli F (1997) Exploring the causes of spatial variation in an assemblage of benthic invertebrates from a submarine cave with sulphur springs. J Exp Mar Biol Ecol 208: 153–168

Bernardini F, Bajaj CL (1997) Sampling and reconstructing manifolds using alpha-shapes. Proc 9th Can Conf Comput Geom (CCCG 1997), Kingston, p 193–198

Bernardini F, Mittleman J, Rushmeier H, Silva C, Taubin G (1999) The ball-pivoting algorithm for surface reconstruction. IEEE Trans Vis Comput Graph 5:349–359

Bibiloni MA, Uriz MJ, Gili JM (1989) Sponge communities in three submarine caves of the Balearic Islands (western Mediterranean): adaptations and faunistic composition. PSZN I: Mar Ecol 10:317–334

Boggus M, Crawfis R (2009) Explicit generation of 3D models of solution caves for virtual environments. In: Arabnia HR, Deligiannidis L (eds) Proc Int Conf Comp Graph & Virt Real (CGVR 2009), 13–16 Jul, CSREA Press, Las Vegas, NV, p 85–90

Bussotti S, Terlizzi A, Fraschetti S, Belmonte G, Boero F (2006) Spatial and temporal variability of sessile benthos in shallow Mediterranean marine caves. Mar Ecol Prog Ser 325:109–119

Chevaldonné P, Lejeusne C (2003) Regional warming-induced species shift in north-west Mediterranean marine caves. Ecol Lett 6:371–379

Cicogna F, Bianchi CN, Ferrari G, Forti P (2003) Grotte marine: cinquant'anni di ricerca in Italia. Ministero dell'Ambiente e della Tutela del Territorio, Rome

Dellow V, Cassie RM (1955) Littoral zonation in two caves in the Auckland district. Trans R Soc NZ 83:321–331

Fairfield N, Kantor G, Wettergreen D (2007) Real-time SLAM with octree evidence grids for exploration in underwater tunnels. J Field Robot 24:3–21

Fichez R (1990) Decrease in allochthonous organic inputs in dark submarine caves, connection with lowering in benthic community richness. Hydrobiologia 207:61–69

Garrabou J, Ballesteros E, Zabala M (2002) Structure and dynamics of north-western Mediterranean rocky benthic communities along a depth gradient. Estuar Coast Shelf Sci 55:493–508

Gerovasileiou V, Voultsiadou E (2012) Marine caves of the Mediterranean Sea: a sponge biodiversity reservoir within a biodiversity hotspot. PLoS ONE 7:e39873

Gili JM, Olivella I, Zabala M, Ros JD (1982) Primera contribución al conocimiento del poblamiento de las cuevas submarinas del litoral catalán. In: Niell FX, Ros JD (eds) Actas del Ier simposio ibérico de estudios del bentos marino. Universidad de Bilbao, San Sebastián, p 818–836

Harmelin JG, Vacelet J (1997) Clues to deep-sea biodiversity in a nearshore cave. Vie Milieu 47:351–354

Harmelin JG, Vacelet J, Vasseur P (1985) Les grottes sous-marines obscures: un milieu extrême et un remarquable biotope refuge. Tethys 11:214–229

Holenstein C, Zlot R, Bosse M (2011) Watertight surface reconstruction of caves from 3D laser data. Proc IEEE Intel Rob Sys (IROS 2011). San Francisco, CA, p 3830–3837

Iliffe TM, Kornicker LS (2009) Worldwide diving discoveries of living fossil animals from the depths of anchialine and marine caves. Smithson Contrib Mar Sci 38:269–280

Jaume D, Boxshall GA (2005) Life in extreme marine environments: anchialine caves. In: Duarte CM (ed) Marine Ecology. Eolss Publishers, Oxford, p 230–250

Laborel J, Vacelet J (1958) Étude des peuplements d'une grotte sous-marine du Golfe de Marseille. Bull Inst Oceanogr 1120:1–20

Lewin J, Woodward JC (2009) Karst geomorphology and environmental change. In: Woodward JC (ed) The physical geography of the Mediterranean. Oxford University Press, Oxford, p 287–317

Martí R, Uriz MJ, Ballesteros E, Turón X (2004) Benthic assemblages in two Mediterranean caves: species diversity and coverage as a function of abiotic parameters and geographic distance. J Mar Biol Assoc UK 84:557–572

Onorato R, Denitto F, Belmonte G (1999) Le grotte marine del Salento: classificazione, localizzazione e descrizione. Thalassia Salent 23:67–116

Parravicini V, Guidetti P, Morri C, Montefalcone M, Donato M, Bianchi CN (2010) Consequences of sea water temperature anomalies on a Mediterranean submarine cave ecosystem. Estuar Coast Mar Sci 86: 276–282

Pérès JM, Picard J (1949) Notes sommaires sur le peuplement des grottes sous-marines de la région de Marseille. CR Soc Biogeogr 227:42–45

Poole DR, Abbot BA, Green RT (2011) Mapping borehole-accessed karst solutional features and culvert conduits using remote sensor technology. Proc IEEE Sensors App Symp, San Antonio, TX, p 29–33

Pouliquen L (1972) Les spongiaires des grottes sous-marines de la région de Marseille. Ecologie et systématique. Tethys 3:717–758

Proctor CJ, Smart PL (1989) A new survey of Kent's cavern, Devon. Proc Univ Bristol Spelaeol Soc 18:422–429

Riedl R (1966) Biologie der Meereshöhlen. Parey, Hamburg

Roff JC, Zacharias MA (2011) Marine conservation ecology. Earthscan, London

Sará M (1962) Zonazione dei Poriferi in biotopi litorali. PSZN I: Mar Ecol 32:44–57

Scheffers SR, de Goeij J, van Duyl FC, Bak RPM (2003) The cave-profiler: a simple tool to describe the 3-D structure of inaccessible coral reef cavities. Coral Reefs 22:49–53

Sellers WI, Chamberlain AT (1998) Ultrasonic cave mapping. J Archaeol Sci 25:867–873

Vacelet J, Boury-Esnault N, Harmelin JG (1994) Hexactinellid cave, a unique deep-sea habitat in the scuba zone. Deep-Sea Res I 41:965–973

Virgilio M, Airoldi L, Abbiati M (2006) Spatial and temporal variations of assemblages in a Mediterranean coralligenous reef and relationships with surface orientation. Coral Reefs 25:265–272

Worthington S (1987) Review of cave surveying techniques. Trans Br Cave Res Assoc 14:56–59

Wunsch M, Richter C (1998) The CaveCam–an endoscopic underwater videosystem for the exploration of cryptic habitats. Mar Ecol Prog Ser 169:277–282

Zabala M, Gili JM (1985) Distribution des Bryozoaires le long d'un gradient sédimentaire dans deux grottes sous-marines du littoral de Majorque. Rapp Comm Int Mer Médit 29:137–140

Zibrowius H (1978) Les Scleractiniaires des grottes sous-marines en Méditerranée et dans l'Atlantique nord-oriental (Portugal, Madère, Canaries, Açores). Pubbl Stn Zool Napoli 40:516–545

Editorial responsibility: Christine Paetzold, Oldendorf/Luhe, Germany

Submitted: November 20, 2012; Accepted: April 12, 2013
Proofs received from author(s): July 9, 2013